Kinetics and Mechanisms of Monolayer Interactions III: Models to Explain Time-Dependent Effects of Injected Cetrimonium Bromide

EDWARD R. GARRETT and FEDERICO A. VILALLONGA ˣ

Abstract □ Two kinetic models are derived to explain the time-dependent effects of cetrimonium ions injected beneath an air–aqueous solution interface without any previously adsorbed or spread monolayer at different ionic strengths. The data show excellent fit and consistency with a multicompartmental kinetic model which postulates a barrier or intermediate compartment between the ionic surfactant in the subphase and the sites on the surface. Such a barrier inhibits free diffusion of the surfactant from the bulk of the solution to these sites. The experimental data are not inconsistent with a model that postulates a time-dependent binding process and the absence of a diffusion-limiting subinterface since, within the limits of the error, the derived rate constants conform to the model prediction that they should be proportional to the surfactant-ion concentration.

Keyphrases □ Monolayer interactions—kinetics and mechanisms for time-dependent effects of cetrimonium bromide injected beneath air–aqueous solution interface without previously adsorbed or spread monolayer at different ionic strengths □ Cetrimonium bromide—kinetics and mechanisms for time-dependent effects after injection beneath air–aqueous solution interface without previously adsorbed or spread monolayer at different ionic strengths

Recent studies on the kinetics and mechanisms of the interaction of phospholipid monolayers at the air–water interface with long hydrocarbon ionic surfactants injected in the subphase demonstrated a time-dependent process for achievement of a final value of surface pressure (1, 2).

The present study describes changes of the surface tension with time after the injection of surfactant ions beneath an air–water interface without any previously adsorbed or spread monolayer and the effect of ionic strength on the adsorption kinetics and final equilibrium surface pressure.

EXPERIMENTAL

Materials—Cetrimonium bromide[1] was the same sample used in previous studies (1, 2). No detectable minimum in the plots of surface tension against the logarithm of the molar concentration was observed. Analytical reagent sodium chloride and potassium chloride were roasted at 650–700° for 6 hr prior to preparation of the aqueous solutions to remove surface-active organic impurities. Deionized, triple-distilled water was used throughout the study. Its pH, after air equilibration, was consistently between 5.6 and 6.0, and its surface tension (γ_0) was within 99.8–100.2% of the value calculated from the Harkin equation (3). The air–water interfacial potential (V_0) was −500 mv (±20 mv).

Instruments and Methods—A 9-cm diameter Teflon dish, provided with two identical micropipets[2] and a Teflon-coated magnetic stirring bar (1.25 × 0.8 cm), was used as a trough in a closed system described previously (1). The final liquid volume in the trough was always 45 ml, corresponding to a liquid depth of 1.58 cm.

Surface tension was measured with a Wilhelmy platinum plate (2.5 × 1.25 × 0.01 cm) attached to an electrobalance[3]. Surface potential was measured with an americium 241 air electrode attached to an electrometer[4]. The outputs of both instruments were fed into a dual-pen recorder[5].

With the platinum plate, the electrodes, and the micropipets in position, water (or the saline solution) was added slowly (42–43 ml) so that it just made contact with the lower edge of the platinum plate (4). After 1 min the surface tension and the interfacial potential were measured and recorded. The liquid volume was adjusted to 45 ml, and the surface tension (γ_0) and interfacial potential (V_0) were measured again. These control values were used for the calculation of the surface pressure ($\Delta\pi$) and surface potential (ΔV) of the final surfactant solution: $\Delta\pi = \gamma_0 - \gamma_s$ and $\Delta V = V_s - V_0$. The subscript s indicates the values that correspond to the surface tension and interfacial potential, respectively, of the final surfactant solution.

A given volume, equal to the volume of the concentrated surfactant solution to be injected, was withdrawn from the dish using the appropriate micropipet. With the other micropipet filled previously with the concentrated surfactant solution, the injection was then started simultaneously with the magnetic stirrer. Within the limits of the experimental error, no significant differences were observed in the $\Delta\pi$ values by stirring 1, 3, 5, or 10 min for a given final concentration. Consequently, after 1 min of stirring, the recording of the surface tension (γ_s) and interfacial potential (V_s) was started. The time necessary for the injection of the desired amount of concentrated surfactant solution was between 10 and 35 sec. The criteria for equilibrium were the constancy of the surface tension (±0.2 dyne cm^{-1}) and the constancy of the interfacial potential (±20 mv) during 30 min. The experiments were performed at 21 ± 1°.

The concentration of the concentrated surfactant solution to be injected was kept below the critical micelle concentration (CMC), and the volumes injected were such as to obtain a final concentration in the 45 ml in the Teflon dish of 8, 4, or 2 μM; at these concentrations, cetrimonium bromide is completely dissociated (5).

At least three different experiments were performed for each final surfactant concentration. The reproducibility was within ±0.5 dyne cm^{-1} for the variation of the surface pressure and ±25 mv for the variation of the surface potential.

RESULTS

The effects of the injection of cetrimonium bromide on the surface pressure ($\Delta\pi$) are compared in Fig. 1 in the absence and in the presence of different concentrations of sodium chloride. In the absence of sodium chloride, the effective changes in the surface pressures were essentially instantaneous processes under the experimental conditions. In the presence of sodium chloride, the equilibrium surface pressure ($\Delta\pi_{eq}$) varied and was a function of the sodium chloride concentration. The rate of achievement of the equilibrium surface pressure was primarily a function of the surfactant-ion concentration in these latter cases.

In all cases, the plot of the reciprocal of the equilibrium surface pressure ($1/\Delta\pi_{eq}$) against the reciprocal ($1/n$) of the final surfactant concentration (n), expressed in molecules per milliliter, gave reasonably straight lines (Fig. 2) within the concentration limits studied.

The substitution of potassium chloride for sodium chloride gave

[1] Eastman Kodak, Rochester, N.Y.
[2] Manostat, New York, N.Y.
[3] Cahn Division, Ventrom Instruments Corp., Paramount, Calif.
[4] Keithley Instruments (610c), Cleveland, Ohio.
[5] Speedomax w/1, Leeds and Northrup, North Wales, Pa.

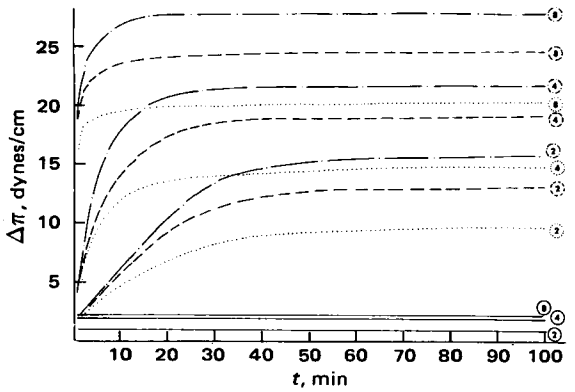

Figure 1—*Effect of the injection of cetrimonium bromide on the surface pressure ($\Delta\pi$) of air–aqueous solution interfaces without any previously adsorbed or spread monolayer. Key: —, water; . . ., 0.15 M NaCl; - - -, 0.30 M NaCl; and - . -., 0.45 M NaCl. Curves are labeled as to micromolar final concentrations of the injected cetrimonium ion.*

similar results. The various $\Delta\pi_{eq}$ values of the several potassium chloride and sodium chloride concentrations are given in Table I.

DISCUSSION

Although it was proposed early (6) that the time dependence of surface tension of surfactant solutions was diffusion dependent, the kinetics of the adsorption processes in many cases could not be explained in terms of simple diffusion alone (7–13) and the concept of a surface potential energy barrier had to be introduced (14–23). These time-dependent processes of adsorption can be quantified by applying the principles of compartmental analysis to a system that is composed of several kinetically distinct compartments.

Model I—Model I postulates a rate-determining process of binding of surfactant ions (S) to a finite number of sites at the interface (I) (Scheme I).

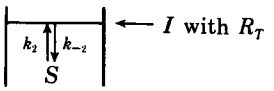

Scheme I

The process can be described by Scheme II:

$$S + R \underset{k_{-2}}{\overset{k_2}{\rightleftharpoons}} (SR)$$

Scheme II

where an amount, S, of surfactant is homogeneously dispersed in a volume, V_s, of solution. The total number of receptor sites at the interface, R_T, is the sum of the amount bound, (SR), and free, R:

$$R_T = R + (SR) \qquad \text{(Eq. 1)}$$

The rate of change of bound sites with time can be formulated as:

$$d(SR)/dt = k_2S(R) - k_{-2}(SR) = k_2S[R_T - (SR)] - k_{-2}(SR) \qquad \text{(Eq. 2)}$$

which can be put into integral form as:

$$\int_0^{(SR)} \frac{d(SR)}{k_2SR_T - (k_2S + k_{-2})(SR)} = \int_{t_0}^{t} dt \qquad \text{(Eq. 3)}$$

If it is postulated that the total number of sites is so small that even when completely saturated, *i.e.*, when $(SR) = (SR_T)$, there is no significant depletion of the surfactant amount in bulk solution so that $S = S_{eq}$, a constant, Eq. 3 can be integrated to:

$$\ln\left[\frac{k_2S_{eq}R_T - [k_2S_{eq} + k_{-2}](SR)}{k_2S_{eq}R_T}\right] = -(k_2S_{eq} + k_{-2})(t - t_0) \qquad \text{(Eq. 4)}$$

and:

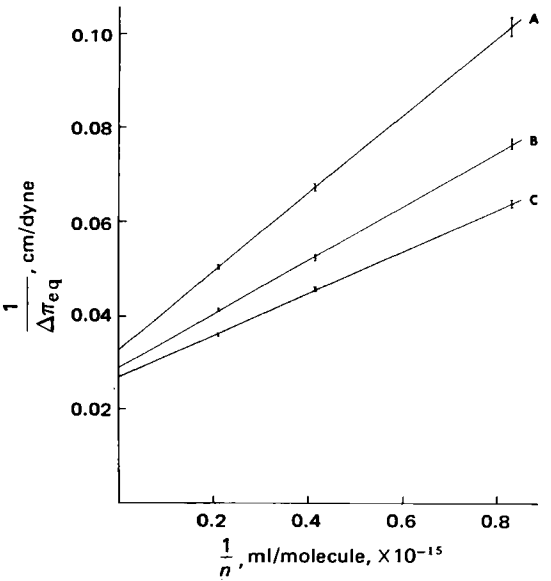

Figure 2—*Typical plots of $1/\Delta\pi_{eq}$ against 1/n for the adsorption of cetrimonium bromide at the air–aqueous solution interfaces, where n is the final surfactant concentration in molecules per milliliter and $\Delta\pi_{eq}$ is the equilibrium surface pressure. Key: A, 0.15 M NaCl; B, 0.30 M NaCl; and C, 0.45 M NaCl.*

$$(SR) = \frac{k_2S_{eq}R_T}{k_2S_{eq} + k_{-2}}[1 - e^{-(k_2S_{eq} + k_{-2})(t - t_0)}] \qquad \text{(Eq. 5)}$$

When final equilibrium is achieved:

$$\lim_{t \to \infty}(SR) = \frac{k_2S_{eq}R_T}{k_2S_{eq} + k_{-2}} = (SR)_{eq} \qquad \text{(Eq. 6)}$$

and:

$$(SR) = (SR)_{eq}[1 - e^{-(k_2S_{eq} + k_{-2})(t - t_0)}] \qquad \text{(Eq. 7)}$$

If the surface pressure ($\Delta\pi$) is proportional to the number of bound sites at the interface, as was postulated previously (24):

$$\Delta\pi = \alpha(SR) \qquad \text{(Eq. 8)}$$

and:

$$(\Delta\pi)_{eq} = \alpha(SR)_{eq} \qquad \text{(Eq. 9)}$$

Equation 7 can be expressed in terms of experimental values as:

$$\Delta\pi = \Delta\pi_{eq}[1 - e^{-(k_2S_{eq} + k_{-2})(t - t_0)}] \qquad \text{(Eq. 10)}$$

or in logarithmic form as:

$$\log(\Delta\pi_{eq} - \Delta\pi) = -\frac{k_2S_{eq} + k_{-2}}{2.303}(t - t_0) + \log \Delta\pi_{eq} \qquad \text{(Eq. 11)}$$

so that a plot of the logarithm of the difference between the final value of the surface pressure ($\Delta\pi_{eq}$) and any value of the surface pressure at a time t should be a straight line of negative slope, m, and intercept $\log \Delta\pi_{eq}$ (Fig. 3*a*) where:

$$-2.303m = k_2S_{eq} + k_{-2} \qquad \text{(Eq. 12)}$$

It follows that m should be a linear function of the amount of surfactant added to a constant volume, V_s, of solution. When the obtained $-m$ values are plotted against surfactant concentration $[S]$:

$$-m = \frac{k_2}{2.303}[S]V_S + \frac{k_{-2}}{2.303} \qquad \text{(Eq. 13)}$$

a straight line should result of slope $V_sk_2/2.303$ and intercept $k_{-2}/2.303$

The plots of $-m$ against the bulk surfactant concentration (Fig. 4) are not inconsistent with Eq. 13 within the limits of concentration studied based on the principles underlying Model I.

Model II—Model II postulates a rate-determining process of diffusion from the bulk solution (B) into the subsurface (S) with

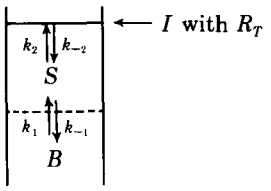

Scheme III

an instantaneous equilibrium with receptor sites (Scheme III). There is strong evidence to postulate the structural ordering of water adjacent to any interface, solid–water, liquid–water, or air–water (24). Particularly in the case of solid–water interfaces (25), anomalous values of thermal expansion, electro- and thermal conductivity, and degeneration of the degree of molecule rotation demand a high degree of ordering for molecules at the interface to produce a new interfacial quasisolid structure.

This model presumes that a compartment exists between the interface (*I*) and the surfactant that is dissolved in the bulk solution. This compartmental model postulates the following compartments.

The Interface (I)—The boundary between the aqueous and the gaseous phases that contains the "active sites" postulated by Langmuir (26).

The Subinterface (S)—A thin region with a thickness of $10–10^3$ water molecule diameters immediately beneath the interface, postulated previously by Ward and Tordai (9). It is further assumed that water molecules are oriented in a given array in this region (25, 27), so that the surfactant must diffuse from a normal homogeneously dispersed solution through this array before it can reach the sites on the interface.

The Bulk Aqueous Phase (B)—The region below the subinterface. Water and solute molecules are distributed at random in this region.

The process can be described by Scheme IV:

$$[B] \underset{k_{-1}}{\overset{k_1}{\rightleftharpoons}} [S] + R \underset{k_{-2}}{\overset{k_2}{\rightleftharpoons}} (SR)$$

Scheme IV

in which $[B]$ and $[S]$ represent the surfactant-ion concentration in the bulk phase and subinterface, respectively; R is the number of active sites per unit of surface area of the interface (I); and (SR) is the number of surfactant ions attached per unit area.

If it is postulated that the interaction of molecules of the surfactant in the subinterface (S) with sites in the interface (I) is instantaneous so that the interaction between S and R in Scheme III is in equilibrium:

$$K_2 = \frac{k_2}{k_{-2}} = \frac{(SR)}{[R][S]} \qquad \text{(Eq. 14)}$$

The fraction, θ, of the total number of sites, R_T, occupied by surfactant molecules is:

$$\theta = \frac{(SR)}{R_T} = \frac{K_2[S]}{1 + K_2[S]} \qquad \text{(Eq. 15)}$$

so that if the surface pressure ($\Delta\pi$) is proportional to the number of bound sites at the interface:

$$\Delta\pi = \alpha(SR) = \alpha\theta R_T = \frac{\alpha R_T K_2[S]}{1 + K_2[S]} = \frac{\Delta\pi_\infty K_2[S]}{1 + K_2[S]} \qquad \text{(Eq. 16)}$$

in which:

$$\Delta\pi_\infty = \alpha R_T \qquad \text{(Eq. 17)}$$

is the maximum value of $\Delta\pi$ that can be achieved with any concentration $[S]$.

If the total number of interface sites, R_T, is relatively small so that $[S]$ is not significantly depleted by binding of the surfactant ions to those sites, the rate of change of surfactant concentration with time from Scheme III is:

$$\frac{d[S]}{dt} = k_1[B] - k_{-1}[S] \qquad \text{(Eq. 18)}$$

As the volume of the subinterface, S, is small with respect to the bulk solution, B, the rise in concentration in the subinterface will not significantly deplete the concentration in the bulk solution; then, for all apparent purposes, $k_1[B]$ is a constant and Eq. 18 may be integrated to give:

$$[S] = \frac{k_1[B]}{k_{-1}}[1 - e^{-k_{-1}(t - t_0)}] \qquad \text{(Eq. 19)}$$

The substitution of this value for $[S]$ in Eq. 16 results in:

$$\Delta\pi = \frac{\frac{\Delta\pi_\infty K_2 k_1[B]}{k_{-1}}[1 - e^{-k_{-1}(t-t_0)}]}{1 + \frac{K_2 k_1[B]}{k_{-1}}[1 - e^{-k_{-1}(t-t_0)}]} = \frac{\Delta\pi_\infty[1 - e^{-k_{-1}(t-t_0)}]}{k_{-1}/K_2 k_1[B] + [1 - e^{-k_{-1}(t-t_0)}]} \qquad \text{(Eq. 20)}$$

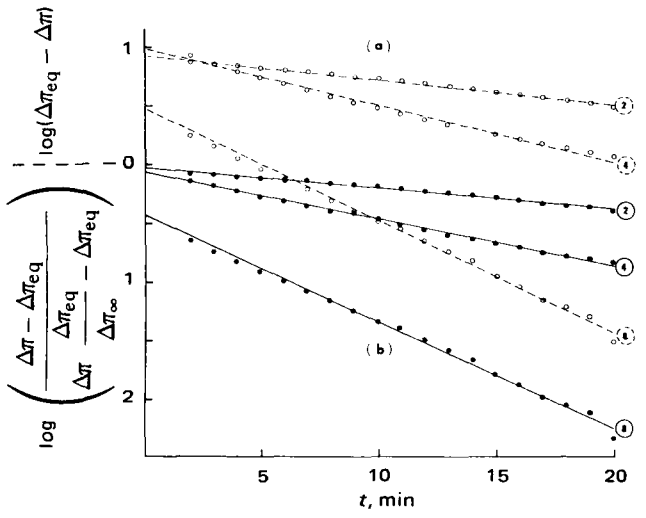

Figure 3—*Plots of log ($\Delta\pi_{eq} - \Delta\pi$) (Model I) and log $\{(\Delta\pi - \Delta\pi_{eq})/[(\Delta\pi)(\Delta\pi_{eq}/\Delta\pi_\infty) - \Delta\pi_{eq}]\}$ (Model II) against time for the adsorption of cetrimonium ions at the air–0.15 M NaCl interface. Lines are labeled as to micromolar final concentration of the injected cetrimonium ions.*

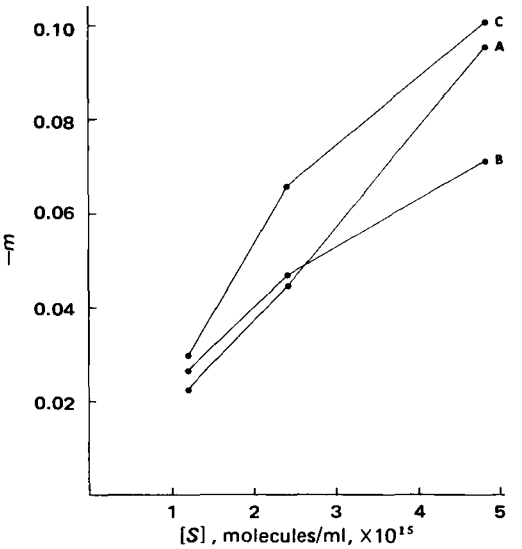

Figure 4—*Plots of −m against the final concentration of cetrimonium ions [S] in molecules per milliliter. Key: A, 0.15 M NaCl; B, 0.30 M NaCl; and C, 0.45 M NaCl.*

Table I—Evaluated Parameters for Adsorption of Various Solution Concentrations of Cetrimonium Ion at the Air–Water Interface for Various Concentrations of Sodium Chloride and Potassium Chloride

		Cetrimonium Ion, Final Concentration					
		2 μM		4 μM		8 μM	
Concentration, M	$\Delta\pi_\infty$, dynes/cm	$\Delta\pi_{eq}$, dynes/cm	k_{-1}, min^{-1}	$\Delta\pi_{eq}$, dynes/cm	k_{-1}, min^{-1}	$\Delta\pi_{eq}$, dynes/cm	k_{-1}, min^{-1}
Sodium chloride							
0.15	30.4	9.9	0.050	14.9	0.086	19.9	0.201
0.30	34.5	13.2	0.050	19.2	0.086	24.2	0.145
0.45	37.1	15.8	0.069	21.8	0.124	27.7	0.218
Potassium chloride							
0.15	30.1	9.8	0.069	14.8	0.108	19.9	0.185
0.30	34.0	13.1	0.066	18.9	0.124	24.1	0.157
0.45	36.6	15.6	0.079	21.7	0.129	27.5	0.248

so that:

$$\lim_{t\to\infty} \Delta\pi = \frac{\Delta\pi_\infty}{1 + k_{-1}/k_1[B]K_2} = \Delta\pi_{eq} \qquad \text{(Eq. 21)}$$

and:

$$\Delta\pi_\infty = \Delta\pi_{eq}\left(1 + \frac{k_{-1}}{k_1[B]K_2}\right) \qquad \text{(Eq. 22)}$$

$$\frac{1}{\Delta\pi_{eq}} = \frac{1}{\Delta\pi_\infty} + \frac{k_{-1}}{k_1K_2\Delta\pi_\infty}\left(\frac{1}{[B]}\right) \qquad \text{(Eq. 23)}$$

so that a plot of the reciprocal of the equilibrium surface pressure ($1/\Delta\pi_{eq}$) against the reciprocal of a particular concentration ($1/[B]$) should be a straight line of positive slope equal to k_{-1}/k_1K_2 ($\Delta\pi_\infty$) and intercept $1/\Delta\pi_\infty$.

When $[1 + (k_{-1}/k_1K_2[B])]$ of Eq. 22 is substituted in Eq. 20:

$$\Delta\pi = \frac{\Delta\pi_\infty(1 - e^{-k_{-1}(t-t_0)})}{\Delta\pi_\infty/\Delta\pi_{eq} - e^{-k_{-1}(t-t_0)}} \qquad \text{(Eq. 24)}$$

and:

$$\frac{\Delta\pi - \Delta\pi_{eq}}{(\Delta\pi)\dfrac{\Delta\pi_{eq}}{\Delta\pi_\infty} - \Delta\pi_{eq}} = e^{-k_{-1}(t-t_0)} \qquad \text{(Eq. 25)}$$

or:

$$\log\left[\frac{\Delta\pi - \Delta\pi_{eq}}{(\Delta\pi)\dfrac{\Delta\pi_{eq}}{\Delta\pi_\infty} - \Delta\pi_{eq}}\right] = \frac{k_{-1}}{2.303}(t - t_0) \qquad \text{(Eq. 26)}$$

so that the logarithmic function for a change in surface pressure from $\Delta\pi$ to its final equilibrium value, $\Delta\pi_{eq}$, when plotted against time should be linear (Fig. 3b) of slope $-k_{-1}/2.303$, where k_{-1} is the first-order rate constant for the return of surfactant from the subinterface to the bulk solution.

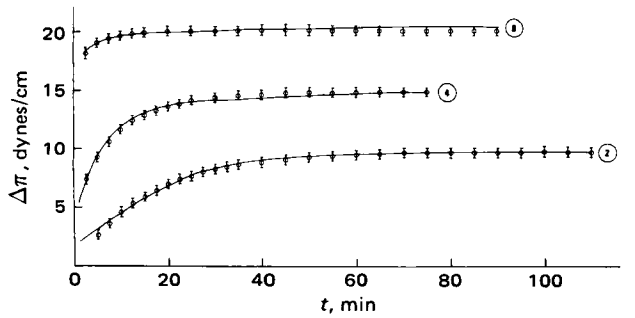

Figure 5—*Plots of surface pressure ($\Delta\pi$) against time (t) for the adsorption of cetrimonium ions at the air–0.15 M NaCl interface; Φ = surface pressures calculated with Eq. 25 (Model II). Curves are labeled as to micromolar final concentrations of the injected surfactant ion.*

The fact that the data conform to Eq. 26 is demonstrated by the linearity of the plots given in Fig. 3b. It was not expected that the data at initial times would conform to Eq. 26, since the agitation of the experimental procedure close to time zero would definitely perturb and accelerate the kinetic processes in the initial moments. When the values of k_{-1} (Table I) obtained from the slopes of the plots are substituted into Eq. 24, the resultant $\Delta\pi$ values fit the $\Delta\pi$–t experimental curves (Fig. 5) excellently within the limits of the experimental error for all saline concentrations studied. Thus, the kinetics of the adsorption of cetrimonium ions at the air–aqueous solution interfaces can be described by the postulation of an intermediate compartment between the interface and the bulk phase.

The product of certain important constants can be estimated from the ratio of the intercept and slope of Eq. 23:

$$\frac{\text{intercept}}{\text{slope}} = \frac{\dfrac{1}{\Delta\pi_\infty}}{\dfrac{k_{-1}}{k_1K_2\Delta\pi_\infty}} = \frac{k_1K_2}{k_{-1}} = K_1K_2 \qquad \text{(Eq. 27)}$$

where $K_1 = k_1/k_{-1}$ and $K_2 = k_2/k_{-2}$ (Scheme IV) are the equilibrium constants of the distributive and surface interaction processes, respectively.

It was shown previously (1, 2) that the energy of activation (ψ) for the process of the interaction of injected cetrimonium ions with a monomolecular layer spread at the air–water interface may be estimated on the assumption that each molecule forming the monolayer constitutes one active site. Thus, the value of (Ns/A) (Eq. 7 of Ref. 1) that represents the number of active sites per square centimeter was given by the known number of molecules necessary to form the monolayer at a given surface pressure.

In the case of an air–water interface without any previously adsorbed or spread monolayer, the term (Ns/A) may be estimated on the basis of the available space per adsorbed surfactant molecule. Molecular models show that the cross-sectional area of the cetrimonium ion is 26.3×10^{-16} cm^2/ion, so that the reciprocal 3.80×10^{14} ions/cm^2 is the maximum number of cetrimonium ions that may exist per square centimeter at the interface at the condition defined by $\Delta\pi = \Delta\pi_\infty$. It is reasonably assumed that this number is

Table II—Estimated Equilibrium Constants for Receptor Site Binding at Interface (K_2) and Partition across a Diffusional Barrier (K_1) and Their Associated Free Energies

Concentration, M	K_1, $\times 10^{-3}$	ΔG_1, kcal/mole	K_2, $\times 10^7$	$\Delta G_2 = \psi$, kcal/mole
Sodium chloride				
0.15	5.96	3.0	3.73	−10.2
0.30	5.91	3.0	4.99	−10.4
0.45	5.83	3.0	6.02	−10.5
Potassium chloride				
0.15	5.95	3.0	3.99	−10.2
0.30	5.93	3.0	5.07	−10.4
0.45	5.88	3.0	6.12	−10.5

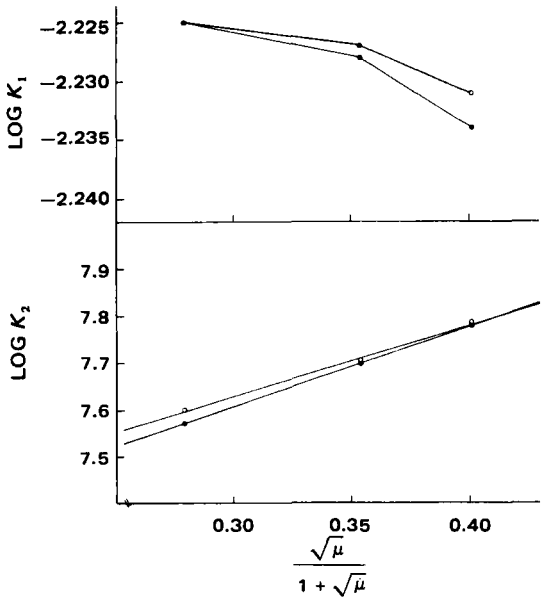

Figure 6—*Plots of log* K_1 *and log* K_2 *against* $[\sqrt{\mu}/(1+\sqrt{\mu})]$ *of the bulk solution. Key:* ●, *sodium chloride; and* ○, *potassium chloride.*

physically equivalent to the number of active sites.

Equation 8 of Ref. 1 can be rewritten in the form:

$$\frac{1}{\Delta\pi_{eq}} = \frac{1}{\Delta\pi_{\infty}} + \frac{(Ns/A)(2\pi m/kT)^{1/2}\nu e^{-\psi/kT}}{\Delta\pi_{\infty}}\left(\frac{1}{n}\right) \quad \text{(Eq. 28)}$$

in which $\Delta\pi_{eq}$ is the equilibrium surface pressure obtained for a final concentration of injected surfactant ion, n (molecules per milliliter); $\Delta\pi_{\infty}$ is the maximum value of $\Delta\pi$ that can be achieved with any final concentration of surfactant ion; (Ns/A) is the number of active sites per square centimeter; π is 3.14 . . . ; m is the absolute mass of the cetrimonium ion; k and T are the Boltzmann constant and the absolute temperature, respectively; ν is the classical frequency of a harmonic oscillator at room temperature (10^{12}/sec); and ψ is the energy of activation of the process of the interaction of cetrimonium ions with active sites at the interface.

The values of ψ obtained for different concentrations of sodium and potassium chlorides on the assumption of $(Ns/A) = 3.80 \times 10^{14}$ active sites/cm^2 are listed in Table II.

The free energy of adsorption per methylene group of a hydrocarbon chain that adsorbs at a clean air–water interface was estimated to be between −0.600 and −0.625 kcal/mole (23, 26, 28, 29). Thus, the value estimated for the hexadecyl hydrocarbon chain of the cetrimonium ion is between −9.6 and −10.0 kcal/mole and compares reasonably with the absolute values of ψ listed in Table II.

The van't Hoff equation:

$$\psi = \Delta G = -RT \ln K \quad \text{(Eq. 29)}$$

permits estimation of the numerical values of K_2 (Table II). It can be observed that these values are a function of the ionic strength of the saline solution in the bulk phase.

Thus, the numerical value of the equilibrium constant K_1 can be estimated from the K_1K_2 value (Eq. 27) and the estimated value of K_2 (Eq. 29). The corresponding free energy values can be calculated from Eq. 29 (Table II). These values do not appear to depend on the ionic strength of the bulk solution.

Effect of Ionic Strength—The experimental values of $\Delta\pi_{\infty}$, $\Delta\pi_{eq}$, and, less consistently, k_{-1} increase with increasing ionic strength (Table I). These facts are reflected in increases of the estimated K_1 and K_2 values with ionic strength (Table II). Log K_1 and log K_2 are plotted against $\sqrt{\mu}/(1+\sqrt{\mu})$ (30), where μ is the ionic strength (Fig. 6).

Such plots of log K_2 were linear with correlation coefficients of 0.99999 and 0.99833 for sodium and potassium chlorides, respectively, whereas the plots of log K_1 showed only small, nonlinear dependence on the ionic strength of the bulk solution. It is reasonable that in this last case the effect of the ionic strength of the bulk solution is counterbalanced by a proportional increase in the ionic strength of the subinterface.

In summary, the following facts are consistent with Model II:

1. The plots of $1/\Delta\pi_{eq}$ against $1/[n]$ are linear as predicted by Eq. 23.
2. The values of k_{-1} estimated from the plot of the logarithmic function of $(\Delta\pi - \Delta\pi_{eq})/[(\Delta\pi)(\Delta\pi_{eq}/\Delta\pi_{\infty}) - \Delta\pi_{eq}]$ against time (Eq. 26) when substituted in Eq. 24 give $\Delta\pi$ values that fit the $\Delta\pi$–t experimental curves excellently between the limits of the experimental error in all saline concentrations studied.
3. The free energy of adsorption estimated from the equilibrium constant K_2 and the van't Hoff equation coincide with those expected from the adsorption of a hexadecyl hydrocarbon chain at the air–water interface.
4. The effect of the ionic strength of the bulk solution on the $\Delta\pi_{\infty}$ and $\Delta\pi_{eq}$ values is consistent with the existence of a subinterface compartment.

The application of this model to the results already obtained with the injection of cetrimonium ions beneath phospholipid monolayers spread at the air–aqueous solution interfaces will be discussed in later papers.

REFERENCES

(1) F. A. Vilallonga, E. R. Garrett, and M. Cereijido, *J. Pharm. Sci.*, **61**, 1720(1972).

(2) F. A. Vilallonga and E. R. Garrett, *ibid.*, **62**, 1605(1973).

(3) "Techniques in Organic Chemistry," 2nd ed., vol. 1, part 1, A. Weissberger, Ed., Interscience, New York, N.Y., 1948, p. 369.

(4) R. Ruyssens, *Rec. Trav. Chim.*, **65**, 580(1946).

(5) D. R. Haydon and J. N. Phillips, *Trans. Faraday Soc.*, **54**, 698(1958).

(6) S. R. Milner, *Phil. Mag.*, **13**, 96(1907).

(7) W. N. Bond and H. O. Puls, *ibid.*, **24**, 864(1937).

(8) S. Ross, *J. Amer. Chem. Soc.*, **67**, 990(1945).

(9) A. F. H. Ward and L. Tordai, *J. Chem. Phys.*, **14**, 453(1946).

(10) K. L. Sutherland, *Aust. J. Sci.*, **A5**, 683(1952).

(11) H. Lange, *Kolloid Z.*, **121**, 130(1951); *ibid.*, **136**, 136(1954).

(12) S. Fordham, *Trans. Faraday Soc.*, **50**, 593(1954).

(13) R. A. Hansen, *J. Phys. Chem.*, **64**, 637(1960); R. A. Hansen, *J. Colloid Sci.*, **16**, 549(1961).

(14) K. S. Doss, *Kolloid Z.*, **86**, 205(1939).

(15) C. M. Blair, Jr., *J. Chem. Phys.*, **16**, 113(1948).

(16) C. C. Addison, *J. Chem. Soc.*, **1944**, 477.

(17) R. Matsuura, H. Kimizuka, S. Miyamoto, R. Shimozawa, and K. Yatsunami, *Bull. Chem. Soc. Jap.*, **32**, 404(1959).

(18) R. Matsuura, H. Kimizuka, and A. Matsubara, *ibid.*, **34**, 1512(1961).

(19) D. J. Salley, A. J. Weith, Jr., A. A. Argyle, and J. K. Dixon, *Proc. Roy. Soc. Ser. A*, **203**, 42(1950).

(20) S. N. Flengas and E. K. Rideal, *Trans. Faraday Soc.*, **55**, 339(1959).

(21) R. Matsuura, H. Kimizuka, S. Miyamoto, and R. Shimozawa, *Bull. Chem. Soc. Jap.*, **31**, 532(1958).

(22) R. Matsuura, H. Kimizuka, A. Matsubara, K. Matsunibu, and T. Matsuda, *ibid.*, **35**, 552(1962).

(23) H. Kimizuka, L. G. Abood, T. Tahara, and V. Kaibara, *J. Colloid Interface Sci.*, **40**, 27(1972).

(24) R. E. Phares, *J. Pharm. Sci.*, **54**, 408(1965).

(25) W. Drost-Hansen, in "Chemistry of the Cell Interface," H. Darrow, Ed., Brown Academic, New York, N.Y., 1971.

(26) I. Langmuir, *J. Amer. Chem. Soc.*, **39**, 1883(1917).

(27) M. S. Metzik, V. D. Perevertaev, V. A. Liopo, G. T. Timostchenko, and A. B. Kiseler, *J. Colloid Interface Sci.*, **43**, 662(1973).

(28) D. E. Woermer and B. S. Snowden, Jr., *Ann. N.Y. Acad. Sci.*, **204**, 113(1973).

(29) D. A. Haydon and F. M. Taylor, *Phil. Trans. Roy. Soc.*, **A252**, 225(1960).

(30) J. Llopis and P. Artalejo, *An. Fis. Quim.*, **58**, 367(1962).

(31) H. S. Harned and B. B. Owen, "Physical Chemistry of

Electrolytic Solutions," 3rd ed., Reinhold, New York, N.Y., 1958, p. 508.

ACKNOWLEDGMENTS AND ADDRESSES

Received November 4, 1974, from the *College of Pharmacy, J. Hillis Miller Health Center, University of Florida, Gainesville, FL 32610*

Accepted for publication March 4, 1975.

The authors are grateful to Mrs. Johanna Hunt for technical collaboration.

[x] To whom inquiries should be directed.

Characterization of Hydrogen Bonding between Selected Barbiturates and Polyethylene Glycol 4000 by IR Spectral Analysis

B. L. CHANG, N. O. NUESSLE, and W. G. HANEY, Jr. [x]

Abstract □ Several barbiturates and primidone were equilibrated with polyethylene glycol 4000 in pyridine. IR spectral properties of these samples indicate that seven disubstituted barbiturates complex with polyethylene glycol 4000 while five disubstituted barbiturates and two trisubstituted barbiturates as well as primidone do not. Forces responsible for complexation of barbiturates with polyethylene glycol 4000, as inferred from spectral data, consist of hydrogen bonds formed between N^1 and N^3 hydrogens of the barbiturate ring and two oxygen atoms of the —O—CH_2CH_2—O— moiety. Also, there appear to be three configurations of intermolecular hydrogen bonding sites between disubstituted barbiturates. Several factors affect the barbiturate–polyethylene glycol 4000 interaction, including the nature of the solvent, C_5 substituents, the number of hydrogen bonds formed between reactants, and the 2-carbonyl group of the barbiturate ring. Complexes of polyethylene glycol 4000 with phenobarbital, butabarbital, and cyclobarbital are stable in water at 26° or below, but complexes of polyethylene glycol 4000 with butethal, cyclopentenyl allylbarbituric acid, pentobarbital, and probarbital are not.

Keyphrases □ Barbiturates—IR characterization of hydrogen bonding with polyethylene glycol 4000 □ Primidone—interaction with polyethylene glycol 4000 □ Hydrogen bonding of barbiturates and primidone with polyethylene glycol—characterized by IR spectrophotometry □ Complexes, barbiturates and polyethylene glycol 4000—IR characterization □ IR spectrophotometry—characterization, hydrogen bonding between barbiturates and polyethylene glycol 4000

Table I—N—H Absorption Bands in Spectra of Barbiturates and Their Complexes

Compound	N—H Absorption Bands, cm^{-1}				
Phenobarbital	3310	3200			3090
Phenobarbital complex	3220			3110	
Pentobarbital		3210	3170		3090
Pentobarbital complex	3240			3110	
Probarbital		3220			3100
Probarbital complex	3270			3120	
Butabarbital		3220			3095
Butabarbital complex	3260			3120	
Cyclobarbital		3220			3100
Cyclobarbital complex	3280			3120	
Butethal		3200			3090
Butethal complex	3220			3100	
Cyclopentenyl allylbarbituric acid		3210	3160		3080
Cyclopentenyl allylbarbituric acid complex		3210			3080

Barbiturates may interact with various organic molecules by hydrogen bonding to form soluble or insoluble complexes such as phenobarbital–theophylline (1), phenobarbital–polyvinylpyrrolidone (2), phenobarbital–caffeine (3), barbital–aminopyrine (4), and phenobarbital–poly-*N*-vinyl-5-methyl-2-oxazolidinone (5). Application of such complexation to pharmaceutics has been discussed in the literature (1–7).

In 1968, Kyogoku *et al.* (8) found that barbiturates also form specific and strong hydrogen bonds to adenine derivatives. Since adenine derivatives exist in a number of biochemicals, *e.g.*, coenzymes and adenosine triphosphate, this interaction formed the basis of a hypothesis explaining the molecular mechanism underlying the pharmacological mode of action of barbiturates. Kyogoku and Yu (9–11) extended the research from ethyladenine to nicotinamide adenine dinucleotide (NAD) and flavine adenine dinucleotide (FAD) and postulated that barbiturates inhibit biological oxidation by interaction with the adenine moiety of NAD and FAD. Thus, an understanding of hydrogen bonding properties is important in barbiturate dosage form development and may allow explanation of the mechanism by which barbiturates inhibit biological oxidation. It is of interest, therefore, to study hydrogen bonding properties of the barbiturate ring in detail.

It was shown (8) that phenobarbital–9-ethyladenine has an association constant of 1200 M^{-1}, whereas barbital–9-ethyladenine and pentobarbital–9-ethyladenine have association constants of 1000 M^{-1}. The larger association constant of phenobarbital–9-ethyladenine was attributed to the lower pKa of phenobarbital (7.3) as compared to that of barbital (7.8) and pentobarbital (8.0). However, since pentobarbital–9-ethyladenine has the same association constant